

A&A manuscript no.
(will be inserted by hand later)

Your thesaurus codes are:
(11.03.1); (12.12.1); (12.03.3)

ESO Imaging Survey

VII. Distant Cluster Candidates over 12 square degrees

M. Scodggio¹, L.F. Olsen^{1,2}, L. da Costa¹, R. Slijkhuis^{1,3}, C. Benoist¹, E. Deul^{1,3}, T. Erben^{1,4}, R. Hook⁵, M. Nonino^{1,6}, A. Wicenc¹, and S. Zaggia^{1,7}

¹ European Southern Observatory, Karl-Schwarzschild-Str. 2, D-85748 Garching b. München, Germany

² Astronomisk Observatorium, Juliane Maries Vej 30, DK-2100 Copenhagen, Denmark

³ Leiden Observatory, P.O. Box 9513, 2300 RA Leiden, The Netherlands

⁴ Max-Planck Institut für Astrophysik, Postfach 1523 D-85748, Garching b. München, Germany

⁵ Space Telescope – European Coordinating Facility, Karl-Schwarzschild-Str. 2, D-85748 Garching b. München, Germany

⁶ Osservatorio Astronomico di Trieste, Via G.B. Tiepolo 11, I-31144 Trieste, Italy

⁷ Osservatorio Astronomico di Capodimonte, via Moiariello 15, I-80131 Napoli, Italy

Received ; accepted

Abstract. In this paper the list of candidate clusters identified from the I-band data of the ESO Imaging Survey (EIS) is completed using the images obtained over a total area of about 12 square degrees. Together with the data reported earlier the total I-band coverage of EIS is 17 square degrees, which has yielded a sample of 252 cluster candidates in the redshift range $0.2 \lesssim z \lesssim 1.3$. This is the largest optically-selected sample currently available in the Southern Hemisphere. It is also well distributed in the sky thus providing targets for a variety of VLT programs nearly year round.

Key words: Galaxies: clusters: general – large-scale structure of the Universe – Cosmology: observations

1. Introduction

The discovery of clusters of galaxies at high redshifts has motivated efforts of compiling lists of candidates for follow-up observations with 8m-class telescopes. The interest in studying these systems spans a broad range of topics and searching for them was identified as one of the primary goals of the ESO Imaging Survey (EIS, Renzini & da Costa 1997), a moderately deep wide-field imaging survey recently conducted at the 3.5m-NTT telescope at La Silla. The main requirements for the cluster search were: 1) to produce a list of candidates large enough to meet the needs of potential VLT programs; 2) to span a broad range of redshifts; 3) to cover a wide range of right ascension thereby allowing the selection of targets year round; 4) to minimize as much as possible spurious detections. These requirements dictated to a large extent the observing strategy adopted by EIS such as the selection

of four fields and the preference given to I-band observations in the second-half of the program. While searches in other wavelengths may provide less contaminated and better defined samples (*e.g.*, IR and X-ray searches), optical searches have the advantage of producing large samples at a faster rate than any other search method, especially with the advent of CCD wide-field imagers.

As stated in Olsen *et al.* (1998a; paper II) the main goal of the EIS cluster search program is to *timely* provide the astronomical community with a list of cluster candidates that can be used as individual targets for follow-up observations in the Southern Hemisphere, especially with the VLT. It must be emphasized that it is not the intention of the present paper to provide a complete and well-defined sample for statistical studies, since such analysis is beyond the scope of the present effort.

The original aim of EIS was to observe about 20 square degrees in four different patches of the sky as described by Renzini and da Costa (1997) (see also Nonino *et al.* 1998, paper I), with a significant fraction of the area covered in V and I-bands. However, as described in earlier papers (paper I, Prandoni *et al.* 1998; paper III) the first-half of the program was severely compromised by bad weather. Therefore, in the second-half, I-band observations covering EIS patches C and D were given priority. The data for these patches are far superior than those of earlier patches and the full coverage of the pre-selected areas was possible, yielding a total area of about 12 square degrees (Benoist *et al.* 1998, paper VI). In this paper the list of cluster candidates found in these regions by using the cluster finding pipeline described in paper II is presented. The results extend the candidate cluster sample presented in papers II and Olsen *et al.* (1998b, paper V), providing targets nearly year round.

Send offprint requests to: M. Scodggio

In section 2 some aspects of the data relevant to the application of the cluster detection algorithm are discussed. In section 3 a list of 198 candidate clusters is presented and the results compared with those of other patches and of the Palomar Distant Cluster Survey (PDCS, Postman *et al.* 1996), currently the only comparable survey. A brief summary is presented in section 4.

2. Galaxy Catalogs

The generation and the characteristics of the EIS galaxy catalogs in patches C and D have been discussed in paper VI. In that paper they were shown to be considerably more homogeneous than those derived from previous patches, with only small variations in depth. As in previous papers, the odd and even catalogs extracted from single exposure images (paper I and II) were independently used to identify clusters of galaxies. This was done by applying the matched filter algorithm described in paper II to six overlapping sections of approximately the same size covering each of the patches considered. For patch C the sections were chosen to avoid a small (~ 0.2 square degree) shallow region mentioned in paper VI. In order to guarantee a full overlap between the regions covered by the odd and even frames the edges of the patches were also trimmed yielding an effective area of 5.3 and 5.5 square degrees for patches C and D, respectively.

The first set of candidate clusters derived from the even and odd frames consisted of over 100 objects in each patch. However, these included an unusually large number of unpaired highly significant detections. The visual inspection of all candidate clusters, together with the even and odd galaxy catalogs, showed that the observed asymmetries were due to the presence of spurious objects detected in the vicinity of bright, saturated stars. As pointed out in paper VI, the reason for this is possibly an electronic problem of the old EMMI controller, when used in the dual-port readout mode. This problem affected the last three runs of EIS by producing faint light trails associated with saturated stars, when these are located in the lower-half part of the detector. Along the trail a large number of spurious, low surface brightness objects are identified, affecting either the odd or even frames in different parts of the sky, but not both simultaneously for the same star. The fraction of these objects is relatively small and they do not significantly affect the number counts or correlation function. However, they have a significant impact in the performance of the matched-filter algorithm which identifies a large number of cluster candidates near bright stars. Since patches C and D are located at low galactic latitudes, with a large number of saturated stars, the frequency of the problem is large, affecting about 50% of the original detections.

Fortunately, the above problem can be partially overcome taking advantage of the sampling strategy of the survey whereby each position on the sky is sampled at least

twice by different parts of the detector (paper I). Since from these single exposures two catalogs are derived, it is possible to overcome the light-trail problem at the catalog level by using, instead of the odd and even catalogs, the catalog which only includes paired galaxies (hereafter, referred to as the paired catalog), detected in both of these catalogs. By construction, this eliminates most spurious objects. The only disadvantage with this procedure is that only one catalog of candidate clusters can be produced and the galaxy sample is slightly shallower. Of course, this solution cannot be applied to samples extracted from the co-added images, which will therefore require some type of correction at the image level. Various alternatives are currently being considered.

3. Catalog of Cluster Candidates

The paired catalogs for the two patches were produced and used as input to the cluster finding pipeline using the same sections and parameters as in the case of the odd/even catalogs. As expected, the use of paired catalogs avoids all cases of cluster candidates that had been detected in the vicinity of light trails and occasionally faint satellite tracks. Note that new candidates are also found, probably because of subtle changes in the background population. It is worth emphasizing that visual inspection of these new candidates shows that they are in general very robust. In order to take advantage of these new detections the final cluster candidate list, shown below, is a combination of all $\geq 3\sigma$ detections derived from the odd/even catalogs, eliminating the spurious detections described in the previous section, supplemented by those derived from the paired catalog.

Table 1 lists 103 cluster candidates in patches C and D detected either at 4σ in one or at 3σ in both odd/even catalogs. These were the objects considered as “good” candidates in papers II and V. Note that 69% of them were also detected using the paired catalog. Table 2 lists the 56 candidates which were detected at 3σ in only one of the even/odd catalogs and in some cases at lower significance in the other. In addition, in contrast to the previous papers, the table also includes 39 candidates, corresponding to 20% of the total sample, which were only detected in the paired catalog. The tables give: in column (1) the identification; in columns (2) and (3) the right ascension and declination in J2000; in column (4) the estimated redshift; in columns (5) and (6) two measures of the cluster richness (see paper II); in columns (7) and (8) the significance of the detection in the even and odd catalogs, respectively; and finally in column (9) the significance of the detection in the paired catalog. In the case of high- z clusters $m_3 + 2$ might exceed the limiting magnitude of the catalog, and no estimate of N_R is possible. These cases are indicated by $N_R = -99$.

In paper II the frequency of noise peaks was estimated to be 0.4 per square degree for the 4σ detections and 4.6

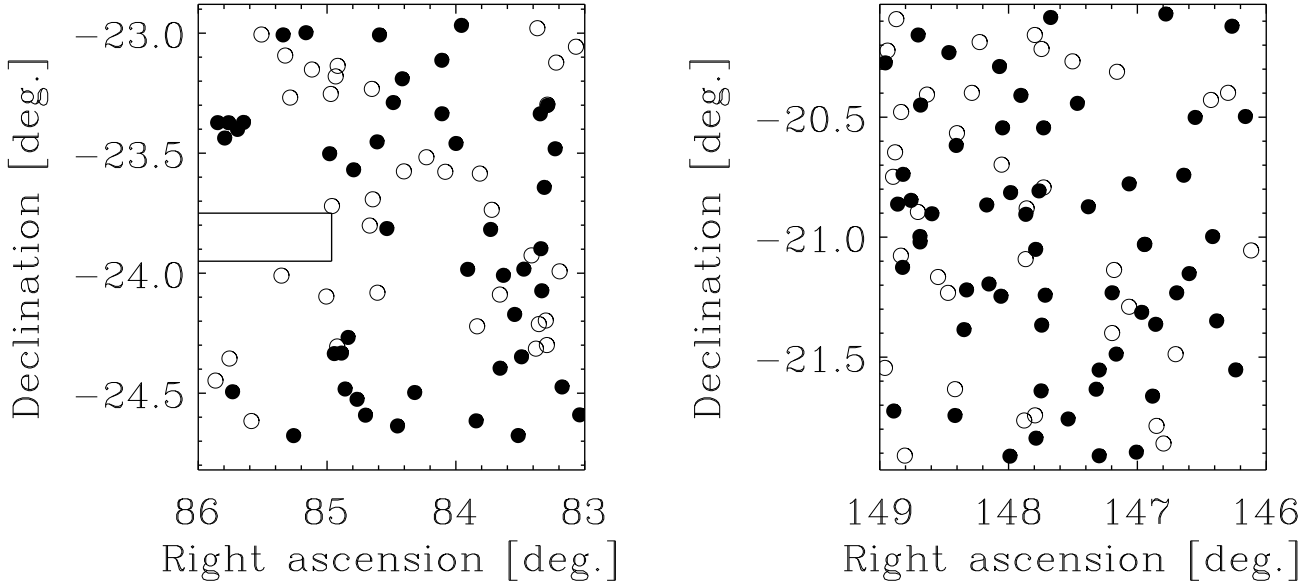


Fig. 1. The projected distributions for the cluster candidates detected in Patches C (left panel) and D (right panel). The filled circles mark the distributions for the “good” candidates as defined in the text. In the distribution for patch C the region discarded from the analysis is indicated.

per square degree for the 3σ detections. Therefore the contamination by spurious detections of the total sample presented in tables 1 and 2 is expected to be $\sim 25\%$ with a significantly smaller frequency if only table 1 is considered.

All detections have been visually inspected and nearly all appear to be promising candidates, although the reliability of the low-redshift candidates is usually more difficult to evaluate. As pointed out above, candidates detected in the paired catalog are particularly encouraging. Furthermore, high-redshift clusters are more frequent in the paired catalog than in the odd/even catalogs. This is probably because the galaxy pairing eliminates faint spurious objects. It should be pointed out that there are also cases where a cluster is detected in either one or both odd/even catalogs but is not detected in the paired catalog. This is possibly due to more subtle effects in the background and noise properties of the maximum likelihood maps. In other cases, especially those detected at relatively high significance in one set but not in the other, the center of the candidate cluster and/or the redshift estimate appear to be incorrect. This is most likely due to projection effects of clusters lying along the line-of-sight, which are not well resolved by the searching algorithm. Finally, note that in patches C and D about 90% of the “good” candidates are detected in both the even and odd catalogs, in contrast to the 65% found in patches A and B. This better matching of detections is because the data for patches C and D are significantly more homogeneous than those of previous patches.

Out of the 198 candidates listed in tables 1 and 2, 93 are in patch C and 105 in patch D, over an effective area of 5.3 and 5.5 square degrees, respectively. The implied number density of clusters is about 18.3 clusters/square degree slightly higher than the values found for patch A and by Postman *et al.* (1996), but similar to the value found for patch B.

The projected distributions of the cluster candidates over the two patches are shown in figure 1. As can be seen in this figure the candidates appear to be distributed uniformly over the whole area of the patches, independently of their significance. Also note that in patch C there are two groupings of cluster candidates, one at $\alpha = 05^h43^m30^s, \delta = -23^\circ25'$ and the other at $\alpha = 05^h40^m00^s, \delta = -24^\circ18'$. In the first case there are three detections at $z \sim 0.2$ and two at $z \sim 0.6 - 0.7$. If confirmed the lower redshift system would be an interesting region for follow-up work. The second system corresponds to an overlap of four systems roughly along the same line-of-sight but with redshifts ranging from 0.2 to 0.6. These systems correspond to the cases with large uncertainties in the position of the center and redshift estimate observed during the visual inspection, as discussed in the previous section.

Figure 2 shows the estimated redshift distribution of the combined sample of candidate clusters identified in patches C and D. The median redshift for this sample is 0.4, which is comparable to the values found for patches A and B. Although a similar median redshift is found for the

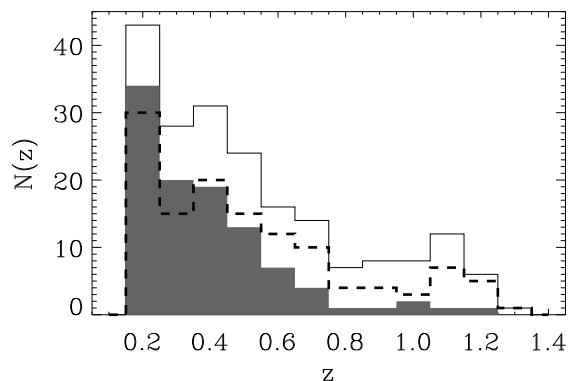


Fig. 2. The redshift distribution for the cluster candidates detected in Patches C and D. The shaded area marks the distribution for the “good” candidates as defined in the text. The dashed line shows the distribution for the candidates detected in the paired catalogs.

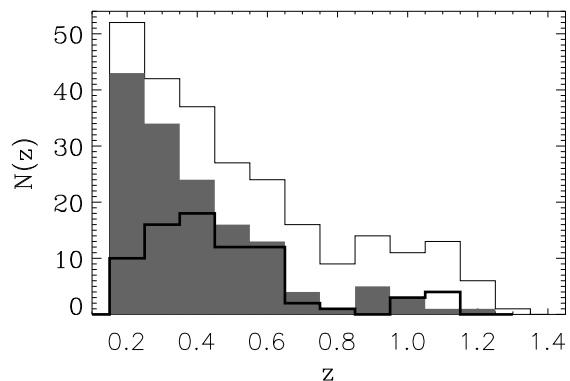


Fig. 3. The redshift distribution of the total sample of EIS clusters (upper panel) as presented in the present work and in Papers II and V in total covering an area of ~ 14.4 square degrees. The thick line shows the estimated redshift distribution of cluster candidates in the PDCS, covering 5.1 square degrees.

candidates obtained from the paired catalog, their redshift distribution (shown in the figure as the dashed line) shows a tail at the high-redshift end ($z \gtrsim 0.8$) in contrast to what is seen for the redshift distribution of the good candidates found in the even/odd catalogs (indicated by the shaded area). Recall that the intrinsic uncertainty of the estimated redshifts is no less than 0.1, due to the discreteness of the filter redshift values (paper II). Furthermore, because of the minimal overlap with clusters with known redshift, the absolute accuracy of the redshift estimates, produced by the cluster finding pipeline, cannot be easily quantified. Therefore the current redshift esti-

mates should be considered tentative, until spectroscopic observations become available.

The total sample of EIS cluster candidates, obtained by combining the detections in the four EIS-wide patches, consists of 252 objects in the redshift range $0.2 \leq z \leq 1.3$. The redshift distribution of the combined sample is shown in figure 3. The median redshift of the distribution is $z \sim 0.4$. Note that the EIS redshift distribution differs somewhat from that observed by PDCS, also shown in the figure. The number of EIS candidates decreases monotonically with redshift up to $z \sim 0.6$ with an extended tail beyond, in contrast to the PDCS which shows a relatively flat distribution peaking at $z \sim 0.4$.

4. Summary

This paper completes the presentation of one of the primary products of EIS, namely a large sample of candidate clusters of galaxies spanning a broad range of redshifts, extending to $z \sim 1$. The candidates were selected in four different patches of the sky covering a large range in right ascension, thereby providing potential targets for VLT which are observable over almost the entire year. Taking all patches together the total sample consists of 252 candidates with about 100 candidates with $z \gtrsim 0.5$. This is by far the largest such a sample currently available and should serve as a good starting point for several programs at the VLT. Note that as emphasized in previous papers of this series the selection criteria adopted has been in general conservative and the primary concern has been the reliability of the candidates rather than completeness of the sample. The catalogs of cluster candidates are available at “<http://www.eso.org/eis>” from where image cutouts from the co-added image can be retrieved for evaluation and preparation of follow-up observations.

Recall that the current cluster candidate lists have been prepared based on galaxy catalogs extracted from the single 150 sec exposures. Since these images are being co-added in the near future it will be possible to extract galaxy catalogs which should reach about 0.5 mag deeper. As soon as these catalogs become available they will also be used to search for clusters and it might be possible to extend somewhat the redshift range of the detected cluster candidates and/or confirm previous detections. However, the available sample is sufficiently large and deep to meet most of the scientific needs in the first year of operation of the VLT.

Acknowledgements. The data presented here were taken at the New Technology Telescope at the La Silla Observatory under the program IDs 59.A-9005(A) and 60.A-9005(A). We thank all the people directly or indirectly involved in the ESO Imaging Survey effort. In particular, all the members of the EIS Working Group for the innumerable suggestions and constructive criticisms. We also thank the ESO Archive Group and ST-ECF for their support. Our special thanks to A. Renzini, VLT Programme Scientist, for his scientific input, support and

dedication in making this project a success. Finally, we would like to thank ESO's Director General Riccardo Giacconi for making this effort possible.

References

- Benoist, C., et al. 1998, submitted to A&A; (Paper VI)
Nonino, M., et al. 1998, submitted to A&A; astro-ph/9803336
(Paper I)
Olsen, L.F., et al. 1998a, submitted to A&A; astro-ph/9803338
(Paper II)
Olsen, L.F., et al. 1998b, submitted to A&A; astro-ph/9807156
(Paper V)
Postman, M., Lubin, L.M., Gunn, J.E., Oke, J.B., Hoessel,
J.G., Schneider, D.P., Christensen, J.A. 1996, AJ, 111, 615
Prandoni, I., et al. 1998, submitted to A&A; astro-ph/9807153
(Paper III)
Renzini, A. & da Costa, L. N. 1997, Messenger 87, 23

Table 1. The 4σ or paired cluster candidates for EIS patches C and D.

Cluster name	α (J2000)	δ (J2000)	z	Λ_{cl}	N_R	σ_{even}	σ_{odd}	σ_{paired}
EIS 0532–2435	05 32 21.7	–24 35 25.3	0.4	49.2	23	3.3	4.1	4.2
EIS 0532–2428	05 32 55.6	–24 28 26.8	0.5	42.2	36	4.2	2.8	3.5
EIS 0533–2328	05 33 8.9	–23 28 54.0	0.4	60.9	62	5.3	5.5	5.6
EIS 0533–2318	05 33 23.5	–23 18 3.8	0.4	35.8	37	3.9	3.7	–
EIS 0533–2338	05 33 29.9	–23 38 33.2	0.4	49.6	45	4.5	4.4	5.2
EIS 0533–2404	05 33 34.7	–24 4 24.1	0.4	57.9	59	4.9	–	–
EIS 0533–2353	05 33 36.5	–23 53 52.9	0.7	72.0	21	3.1	3.3	3.6
EIS 0533–2320	05 33 37.6	–23 20 9.5	0.3	36.7	38	4.4	4.0	4.7
EIS 0534–2358	05 34 9.2	–23 58 59.6	0.6	71.6	22	3.6	3.9	4.2
EIS 0534–2420	05 34 13.7	–24 20 54.5	0.2	42.1	10	6.0	6.6	–
EIS 0534–2440	05 34 20.1	–24 40 35.5	0.4	54.1	54	4.5	4.5	4.6
EIS 0534–2410	05 34 26.9	–24 10 19.1	0.3	40.2	40	3.6	5.5	4.6
EIS 0534–2400	05 34 48.5	–24 0 32.4	0.2	31.0	29	5.2	5.0	5.9
EIS 0534–2423	05 34 55.0	–24 23 45.5	0.2	41.4	26	7.9	6.4	6.9
EIS 0535–2349	05 35 13.2	–23 49 4.2	0.4	49.1	30	4.3	3.7	4.6
EIS 0535–2436	05 35 41.1	–24 36 55.1	0.3	35.8	23	3.9	4.2	–
EIS 0535–2359	05 35 57.4	–23 59 2.7	0.8	151.5	31	3.7	4.3	–
EIS 0536–2258	05 36 9.4	–22 58 3.2	1.1	210.8	–99	3.8	3.0	3.1
EIS 0536–2327	05 36 19.8	–23 27 34.5	0.3	54.4	26	8.2	5.1	7.7
EIS 0536–2320	05 36 46.9	–23 20 8.8	0.4	34.7	21	3.7	3.0	–
EIS 0536–2306	05 36 47.1	–23 6 46.6	0.2	19.7	23	5.2	5.4	5.8
EIS 0537–2429	05 37 39.4	–24 29 50.1	0.5	43.0	40	3.2	3.2	–
EIS 0538–2311	05 38 3.2	–23 11 24.2	0.6	99.3	87	6.9	6.7	7.3
EIS 0538–2438	05 38 12.4	–24 38 11.4	0.3	38.1	27	4.4	4.6	5.1
EIS 0538–2317	05 38 20.6	–23 17 20.7	0.7	81.7	109	2.9	4.2	–
EIS 0538–2348	05 38 33.0	–23 48 50.5	0.7	74.6	83	4.2	3.4	3.1
EIS 0538–2300	05 38 47.1	–23 0 26.4	0.5	44.4	19	3.0	3.5	3.9
EIS 0538–2327	05 38 51.7	–23 27 10.4	0.2	26.8	19	5.8	8.0	–
EIS 0539–2435	05 39 14.0	–24 35 30.0	0.2	32.8	19	4.6	5.1	5.0
EIS 0539–2431	05 39 30.3	–24 31 32.2	0.4	49.9	54	4.5	4.4	4.6
EIS 0539–2334	05 39 36.9	–23 34 9.3	0.2	26.7	23	5.8	5.1	–
EIS 0539–2416	05 39 47.5	–24 16 3.8	0.3	31.5	17	3.9	3.0	–
EIS 0539–2428	05 39 53.3	–24 28 57.4	0.6	71.8	24	3.7	3.8	4.3
EIS 0540–2419	05 40 0.3	–24 19 58.6	0.2	33.7	22	5.0	5.4	6.1
EIS 0540–2420	05 40 14.0	–24 20 6.1	0.4	40.3	11	–	4.2	–
EIS 0540–2330	05 40 23.1	–23 30 8.1	0.3	31.5	41	4.1	3.4	–
EIS 0541–2259	05 41 8.6	–22 59 53.0	0.2	37.5	68	0.0	6.3	9.6
EIS 0541–2440	05 41 32.4	–24 40 36.8	0.5	67.1	45	4.1	3.2	3.9
EIS 0541–2300	05 41 52.6	–23 0 25.9	0.2	32.6	37	5.7	4.5	–
EIS 0543–2322	05 43 8.9	–23 22 18.6	0.3	31.6	15	4.1	3.9	–
EIS 0543–2324	05 43 20.3	–23 24 3.5	0.2	24.2	30	4.2	5.5	–
EIS 0543–2429	05 43 29.9	–24 29 38.7	0.2	30.4	36	5.3	4.7	5.8
EIS 0543–2322	05 43 37.6	–23 22 22.9	0.7	81.5	48	4.1	–	–
EIS 0543–2326	05 43 45.2	–23 26 13.1	0.6	68.9	42	2.9	4.3	3.3
EIS 0543–2322	05 43 58.6	–23 22 22.1	0.2	30.0	9	5.3	–	–
EIS 0946–2029	09 46 12.8	–20 29 49.9	0.2	72.8	44	9.1	8.6	8.6
EIS 0946–2133	09 46 31.1	–21 33 10.8	0.2	33.8	21	4.5	4.9	4.4
EIS 0946–2007	09 46 38.1	–20 7 16.0	0.5	131.1	55	7.8	–	3.1
EIS 0947–2120	09 47 6.9	–21 20 55.7	0.2	43.7	50	5.8	5.5	6.2
EIS 0947–2059	09 47 14.5	–20 59 51.0	0.3	32.5	26	3.5	3.5	–
EIS 0947–2030	09 47 47.3	–20 30 4.0	1.0	133.3	23	3.1	3.2	3.6
EIS 0947–2109	09 47 58.6	–21 9 6.2	0.2	27.2	14	4.0	5.4	5.2
EIS 0948–2044	09 48 8.8	–20 44 31.2	0.2	43.4	32	5.5	5.9	6.0
EIS 0948–2113	09 48 22.1	–21 13 55.0	0.3	41.2	53	4.7	–	–
EIS 0948–2004	09 48 42.5	–20 4 12.7	1.2	257.8	–99	4.1	2.6	5.3
EIS 0949–2121	09 49 1.7	–21 21 47.2	0.4	66.7	25	5.3	3.3	3.5

Table 1. Continued.

Cluster name	α (J2000)	δ (J2000)	z	Λ_{cl}	N_R	σ_{even}	σ_{odd}	σ_{paired}
EIS 0949–2139	09 49 7.5	–21 39 44.6	0.6	116.7	80	5.1	–	–
EIS 0949–2101	09 49 22.1	–21 1 47.1	0.3	37.7	57	3.6	3.9	4.0
EIS 0949–2101	09 49 22.9	–21 1 50.1	0.3	29.3	25	3.5	3.2	3.7
EIS 0949–2118	09 49 28.0	–21 18 47.6	0.4	40.7	45	3.3	3.0	–
EIS 0949–2153	09 49 38.0	–21 53 44.6	0.9	129.3	32	3.6	3.3	3.4
EIS 0949–2046	09 49 51.5	–20 46 40.6	0.2	48.8	24	5.2	5.3	5.4
EIS 0950–2129	09 50 16.0	–21 29 14.0	0.4	43.1	32	3.4	3.5	–
EIS 0950–2113	09 50 23.6	–21 13 54.3	0.4	57.3	43	4.8	4.0	–
EIS 0950–2154	09 50 47.9	–21 54 39.0	0.5	69.4	33	3.5	4.2	4.0
EIS 0950–2133	09 50 48.0	–21 33 13.1	0.2	31.5	10	4.1	3.5	4.4
EIS 0950–2138	09 50 53.6	–21 38 0.7	0.5	54.2	27	–	4.1	–
EIS 0951–2052	09 51 8.3	–20 52 23.6	0.2	31.9	16	3.4	3.2	–
EIS 0951–2026	09 51 28.9	–20 26 33.0	0.2	44.2	13	4.3	4.9	4.7
EIS 0951–2145	09 51 46.4	–21 45 27.1	0.2	62.0	42	8.1	7.7	7.7
EIS 0952–2005	09 52 19.3	–20 5 4.7	0.4	65.1	37	4.5	4.4	4.5
EIS 0952–2114	09 52 29.5	–21 14 30.6	0.3	38.7	35	2.6	4.2	–
EIS 0952–2032	09 52 32.6	–20 32 40.0	0.3	106.9	156	9.0	9.7	9.3
EIS 0952–2121	09 52 36.1	–21 21 59.6	0.4	72.8	31	4.9	5.8	5.0
EIS 0952–2138	09 52 37.3	–21 38 25.6	0.4	52.1	33	4.2	4.4	4.6
EIS 0952–2048	09 52 41.1	–20 48 25.9	0.4	55.5	37	3.0	4.5	–
EIS 0952–2150	09 52 46.8	–21 50 15.1	0.2	33.8	28	2.8	4.4	–
EIS 0952–2103	09 52 47.5	–21 3 3.1	0.2	33.4	11	3.6	3.2	–
EIS 0953–2054	09 53 6.0	–20 54 17.3	0.2	50.2	6	5.4	4.9	–
EIS 0953–2024	09 53 15.3	–20 24 33.5	0.3	63.8	33	6.2	6.9	6.6
EIS 0953–2048	09 53 34.6	–20 48 51.7	0.3	46.2	49	6.2	–	5.5
EIS 0953–2154	09 53 35.8	–21 54 44.7	0.3	54.5	20	4.3	5.7	–
EIS 0953–2032	09 53 49.7	–20 32 40.0	0.3	35.1	25	3.5	3.8	4.0
EIS 0953–2114	09 53 52.7	–21 14 46.1	1.0	172.1	59	3.1	3.4	3.6
EIS 0953–2017	09 53 55.5	–20 17 20.3	0.2	36.1	14	5.2	4.6	5.6
EIS 0954–2111	09 54 15.3	–21 11 42.1	0.5	73.2	66	5.1	–	5.8
EIS 0954–2051	09 54 19.5	–20 51 57.1	0.5	62.2	34	3.9	3.2	3.6
EIS 0954–2113	09 54 57.5	–21 13 11.2	0.5	96.5	82	6.2	4.3	5.2
EIS 0955–2123	09 55 2.3	–21 23 6.7	0.2	53.3	26	6.9	7.5	7.5
EIS 0955–2037	09 55 16.9	–20 37 4.1	0.2	37.1	37	5.3	4.1	4.7
EIS 0955–2144	09 55 19.2	–21 44 34.5	0.6	85.0	107	4.3	4.3	4.0
EIS 0955–2013	09 55 30.7	–20 13 51.1	0.5	51.9	31	3.1	3.2	3.8
EIS 0956–2054	09 56 2.7	–20 54 8.6	0.2	38.1	28	5.5	5.0	5.6
EIS 0956–2026	09 56 24.0	–20 26 58.7	0.2	31.8	19	4.6	4.6	5.6
EIS 0956–2101	09 56 24.9	–21 1 11.7	0.4	53.4	22	4.3	4.0	4.5
EIS 0956–2059	09 56 25.2	–20 59 49.8	0.3	39.7	37	4.7	4.5	4.8
EIS 0956–2009	09 56 28.6	–20 9 27.4	0.5	58.2	22	3.5	3.0	3.9
EIS 0956–2050	09 56 42.0	–20 50 47.9	0.2	27.2	48	2.8	6.5	–
EIS 0956–2044	09 56 56.9	–20 44 17.7	0.5	96.0	61	3.1	6.0	–
EIS 0956–2107	09 56 57.9	–21 7 33.3	0.3	30.1	51	3.0	3.6	4.0
EIS 0957–2051	09 57 7.2	–20 51 44.3	0.2	27.9	36	4.0	4.9	–
EIS 0957–2143	09 57 14.5	–21 43 27.5	0.2	51.2	23	6.0	7.2	6.7
EIS 0957–2016	09 57 30.3	–20 16 25.5	0.6	96.7	47	5.6	–	–

Table 2. 3σ cluster candidates for EIS patches C and D.

Cluster name	α (J2000)	δ (J2000)	z	Λ_{cl}	N_R	σ_{even}	σ_{odd}	σ_{paired}
EIS 0532–2303	05 32 28.9	–23 3 23.1	1.1	191.5	–99	–	–	3.0
EIS 0533–2359	05 33 0.3	–23 59 32.5	0.7	81.0	22	–	–	3.3
EIS 0533–2307	05 33 6.9	–23 7 21.1	1.2	283.7	–99	–	–	3.5
EIS 0533–2317	05 33 24.0	–23 17 52.3	0.7	92.1	35	–	–	4.5
EIS 0533–2417	05 33 24.8	–24 17 58.1	0.4	33.0	26	–	–	3.2
EIS 0533–2411	05 33 26.9	–24 11 50.3	0.5	47.7	24	–	–	3.3
EIS 0533–2412	05 33 40.3	–24 12 43.8	1.1	299.2	72	–	–	3.3
EIS 0533–2441	05 33 41.5	–24 41 51.8	0.7	77.2	86	3.0	2.8	–
EIS 0533–2258	05 33 43.2	–22 58 45.4	0.9	107.3	46	3.1	–	–
EIS 0533–2418	05 33 46.0	–24 18 52.1	0.5	70.3	66	–	–	5.2
EIS 0533–2355	05 33 54.4	–23 55 33.1	0.8	86.9	84	–	–	3.5
EIS 0534–2430	05 34 12.5	–24 30 17.9	1.0	173.4	–99	3.0	2.9	–
EIS 0534–2405	05 34 55.3	–24 5 20.6	0.7	81.1	54	–	–	3.3
EIS 0535–2402	05 35 7.4	–24 2 28.4	0.4	46.3	45	2.6	3.9	–
EIS 0535–2344	05 35 11.0	–23 44 9.6	1.2	282.6	12	–	–	3.5
EIS 0535–2335	05 35 33.9	–23 35 6.2	0.3	31.5	18	3.8	–	–
EIS 0535–2413	05 35 39.1	–24 13 17.0	0.5	47.8	37	–	3.1	–
EIS 0535–2302	05 35 46.4	–23 2 9.2	0.3	31.6	30	2.7	3.8	–
EIS 0536–2334	05 36 40.4	–23 34 39.3	0.5	42.5	29	3.3	–	–
EIS 0537–2331	05 37 16.8	–23 31 1.0	0.2	44.6	31	–	–	10.2
EIS 0537–2354	05 37 17.9	–23 54 46.2	0.8	83.3	29	3.7	2.6	3.4
EIS 0537–2444	05 37 28.0	–24 44 18.8	0.3	22.6	6	3.0	2.6	–
EIS 0538–2334	05 38 0.1	–23 34 33.0	1.1	173.9	–99	–	3.0	–
EIS 0538–2405	05 38 5.1	–24 5 6.8	0.8	100.2	44	3.0	2.8	3.2
EIS 0538–2345	05 38 12.0	–23 45 6.2	0.9	97.5	43	3.3	2.8	–
EIS 0538–2331	05 38 48.0	–23 31 41.1	0.5	37.4	16	2.8	3.1	–
EIS 0538–2304	05 38 49.0	–23 4 10.2	0.7	61.8	37	2.9	3.0	3.3
EIS 0538–2404	05 38 51.0	–24 4 53.0	1.1	255.6	–99	–	3.5	–
EIS 0539–2341	05 39 –	–23 41 31.7	0.6	47.0	38	–	–	3.2
EIS 0539–2313	05 39 1.8	–23 13 56.0	0.4	31.3	17	–	–	3.7
EIS 0539–2348	05 39 5.8	–23 48 5.8	0.2	64.1	23	–	–	14.6
EIS 0540–2308	05 40 7.6	–23 8 10.4	0.7	87.5	56	–	–	3.7
EIS 0540–2418	05 40 8.5	–24 18 19.3	0.6	83.8	40	–	–	4.9
EIS 0540–2310	05 40 11.4	–23 10 48.3	0.4	30.8	37	–	–	3.4
EIS 0540–2343	05 40 18.5	–23 43 13.1	0.6	64.0	12	–	3.4	–
EIS 0540–2315	05 40 20.8	–23 15 11.5	0.7	79.2	32	–	–	3.3
EIS 0540–2405	05 40 29.4	–24 5 50.1	0.2	27.5	17	–	–	5.0
EIS 0540–2309	05 40 57.1	–23 9 4.8	0.6	60.9	36	–	–	3.3
EIS 0541–2437	05 41 15.2	–24 37 32.0	0.5	48.0	63	2.5	3.0	–
EIS 0541–2432	05 41 16.8	–24 32 32.1	0.4	44.4	40	3.7	2.9	3.1
EIS 0541–2316	05 41 39.0	–23 16 6.2	0.2	38.3	25	–	–	7.3
EIS 0541–2305	05 41 48.6	–23 5 35.5	0.8	89.6	52	–	–	3.1
EIS 0541–2400	05 41 55.8	–24 0 36.7	1.2	489.5	–99	–	–	4.7
EIS 0542–2300	05 42 34.3	–23 0 20.1	0.3	35.2	21	–	–	4.8
EIS 0542–2436	05 42 53.6	–24 36 57.7	0.2	34.1	13	–	–	5.8
EIS 0543–2359	05 43 29.6	–23 59 51.7	1.1	243.1	–99	3.2	2.9	3.9
EIS 0543–2421	05 43 35.8	–24 21 20.3	1.0	167.7	22	–	3.1	–
EIS 0544–2426	05 44 2.8	–24 26 51.0	0.2	33.3	28	–	–	5.6
EIS 0945–2005	09 45 58.0	–20 5 38.5	0.9	124.2	62	2.7	3.7	3.5
EIS 0946–2103	09 46 2.0	–21 3 18.9	1.0	152.5	45	3.9	–	–
EIS 0946–2053	09 46 5.2	–20 53 41.5	0.6	66.5	49	3.3	2.9	3.5
EIS 0946–2023	09 46 45.4	–20 23 54.8	0.3	36.7	30	3.9	–	–
EIS 0947–2044	09 47 17.4	–20 44 5.0	0.9	103.6	39	2.7	3.4	3.3
EIS 0947–2025	09 47 17.6	–20 25 41.8	0.9	113.9	60	–	3.1	–
EIS 0947–2057	09 47 34.9	–20 57 24.3	0.4	43.9	29	2.7	3.5	–
EIS 0948–2123	09 48 17.5	–21 23 33.3	0.4	40.5	26	2.9	3.0	3.1

Table 2. Continued.

Cluster name	α (J2000)	δ (J2000)	z	Λ_{cl}	N_R	σ_{even}	σ_{odd}	σ_{paired}
EIS 0948–2129	09 48 24.1	–21 29 14.8	0.7	80.7	36	3.2	–	–
EIS 0948–2151	09 48 46.8	–21 51 34.7	1.0	203.7	–99	3.4	–	3.1
EIS 0949–2147	09 49 0.0	–21 47 10.7	1.1	239.3	76	–	–	3.4
EIS 0949–2058	09 49 32.6	–20 58 29.5	0.5	58.2	63	2.9	3.3	3.2
EIS 0949–2117	09 49 51.6	–21 17 24.1	0.5	63.1	88	–	3.9	–
EIS 0950–2103	09 50 8.0	–21 3 40.7	0.2	23.8	2	3.3	2.6	–
EIS 0950–2018	09 50 14.4	–20 18 39.2	1.1	170.6	–99	–	3.5	–
EIS 0950–2108	09 50 19.9	–21 8 12.0	1.1	192.4	40	–	–	3.1
EIS 0950–2123	09 50 23.5	–21 23 58.2	0.6	60.2	39	–	–	3.2
EIS 0951–2146	09 51 3.8	–21 46 8.9	0.6	53.4	20	3.3	2.7	3.3
EIS 0951–2102	09 51 30.8	–21 2 54.4	0.4	49.4	35	3.4	2.7	3.0
EIS 0951–2046	09 51 31.8	–20 46 56.6	0.5	65.1	25	3.5	2.7	3.3
EIS 0951–2016	09 51 38.1	–20 16 2.8	1.3	321.6	–99	–	–	3.7
EIS 0952–2047	09 52 32.5	–20 47 34.1	0.7	79.6	49	–	–	3.1
EIS 0952–2012	09 52 36.3	–20 12 57.2	1.1	168.7	–99	–	3.4	–
EIS 0952–2144	09 52 48.7	–21 44 32.6	0.2	36.1	41	–	–	4.7
EIS 0952–2009	09 52 49.0	–20 9 27.2	0.9	93.0	17	–	–	3.2
EIS 0953–2052	09 53 4.4	–20 52 48.5	0.2	38.9	19	–	–	4.2
EIS 0953–2105	09 53 6.3	–21 5 29.2	1.0	186.0	–99	3.8	–	–
EIS 0953–2145	09 53 9.0	–21 45 49.7	0.3	31.2	14	–	–	3.4
EIS 0953–2041	09 53 51.5	–20 41 52.1	0.4	41.5	49	–	3.6	–
EIS 0954–2120	09 54 1.2	–21 20 3.2	0.9	110.4	42	2.5	3.1	–
EIS 0954–2011	09 54 32.8	–20 11 13.3	0.8	91.6	21	–	3.6	–
EIS 0954–2023	09 54 47.5	–20 23 55.2	1.1	217.9	52	–	–	3.3
EIS 0955–2033	09 55 15.5	–20 33 59.8	0.4	42.4	31	–	–	3.8
EIS 0955–2137	09 55 19.1	–21 37 59.7	0.5	43.6	36	–	–	3.0
EIS 0955–2113	09 55 32.3	–21 13 55.3	0.6	68.2	67	–	3.2	–
EIS 0955–2008	09 55 36.3	–20 8 26.2	1.0	153.3	26	3.2	2.6	–
EIS 0955–2109	09 55 51.1	–21 9 57.4	0.7	71.5	67	–	–	3.1
EIS 0956–2024	09 56 11.9	–20 24 21.2	1.2	252.7	–99	3.0	–	–
EIS 0956–2053	09 56 29.0	–20 53 41.6	0.4	40.3	25	3.5	–	3.4
EIS 0956–2154	09 56 53.6	–21 54 36.5	0.4	35.5	15	–	–	3.3
EIS 0957–2028	09 57 0.6	–20 28 42.6	0.8	85.7	40	3.2	–	–
EIS 0957–2104	09 57 1.0	–21 4 37.6	1.1	188.9	25	3.1	–	–
EIS 0957–2005	09 57 9.6	–20 5 29.4	1.2	256.6	–99	3.2	–	3.7
EIS 0957–2038	09 57 11.9	–20 38 46.6	0.5	58.8	9	3.6	–	–
EIS 0957–2044	09 57 15.8	–20 44 54.4	0.3	36.1	17	3.9	–	–
EIS 0957–2013	09 57 26.2	–20 13 21.5	0.6	62.3	28	–	–	3.5
EIS 0957–2132	09 57 31.0	–21 32 40.9	0.3	38.3	6	–	–	4.2